

Supporting Information

Gas phase mechanisms of degradation of toxic organophosphorus compounds: do they follow a common pattern of alkaline hydrolysis reaction as in phosphotriesterase?

Edyta Dyguda–Kazimierowicz, W. Andrzej Sokalski,*

Department of Chemistry, Wrocław University of Technology

Wyb. Wyspiańskiego 27, 50–370 Wrocław, Poland

and Jerzy Leszczyński

Jackson State University, Jackson, Mississippi, USA

Contents

Hydrolysis of a model compound	S2
Hydrolysis of demeton–S	S4
Comparison of geometries for A and B paths	S5
Solvent–induced effects	S13
Animation of the reaction pathways	S16

*tel./fax +48 71 320 2457; sokalski@pwr.wroc.pl

Hydrolysis of a model compound

To establish and validate the most cost-effective model chemistry, the HF/6-31+G(d) structures associated with a reaction coordinate for the alkaline hydrolysis of *O,O*-dimethyl phosphorofluoridate were further reoptimized at MP2/6-311++G(d,p) level of theory. While only minor changes in geometrical parameters occurred with the increase of the complexity of theory (see Table S1 for the comparison of selected bond lengths), the corresponding energies differed significantly. Apparently, electron correlation effects are important in the evaluation of energy, but neglecting them in geometry optimization results in still reasonable structures. To test this hypothesis, MP2/6-311++G(d,p) energies were calculated for HF-optimized structures. Similarity of both sets of the results (Table S2) indicates the possibility of using such an approach in case of organophosphate compounds with bulkier substituents that make it difficult to perform calculations at higher level of theory.

Table S1: Comparison of selected TS1a interatomic distances (in the units of Å; angles in degrees) for the structures optimized at different levels of theory: HF/6-31+G(d) and MP2/6-311++G(d,p). Designation of atoms as in Figure S1.

Distances (angle)	HF	MP2
P-O	2.740	2.830
P-F	1.592	1.620
P-O-H	103	102
P-O1	1.454	1.476
P-O2	1.563	1.590
P-O3	1.563	1.590

Figure S1: Designation of TS1a atoms.

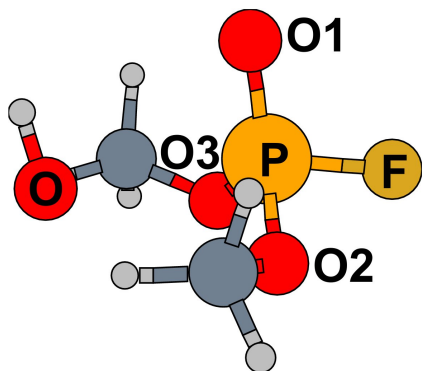


Table S2: Comparison of the activation energies (kcal · mol⁻¹) for the alkaline hydrolysis of *O,O*-dimethyl phosphorofluoridate (A and B paths).

Step	ΔE^a		ΔG	
	MP2 ^b	MP2//HF ^c	MP2	MP2//HF
INT1→TS1a	3.2	3.6	4.3	4.8
INT1→TS1b	5.0	5.4	6.5	7.2
INT2a→TSr1a	2.7	2.5	2.7	3.0
INT2b→TSr1b	0.7	0.7	1.2	1.1
INT3→TSr2a	3.1	3.1	3.3	3.6
INT3→TSr2b	4.1	4.1	4.7	4.7
INT4a→TS2a	5.6	4.8	5.2	4.4
INT4b→TS2b	5.0	4.4	4.6	4.4

^a ΔE corresponds to the sum of electronic and zero-point energies; ΔG stands for the Gibbs free energy.

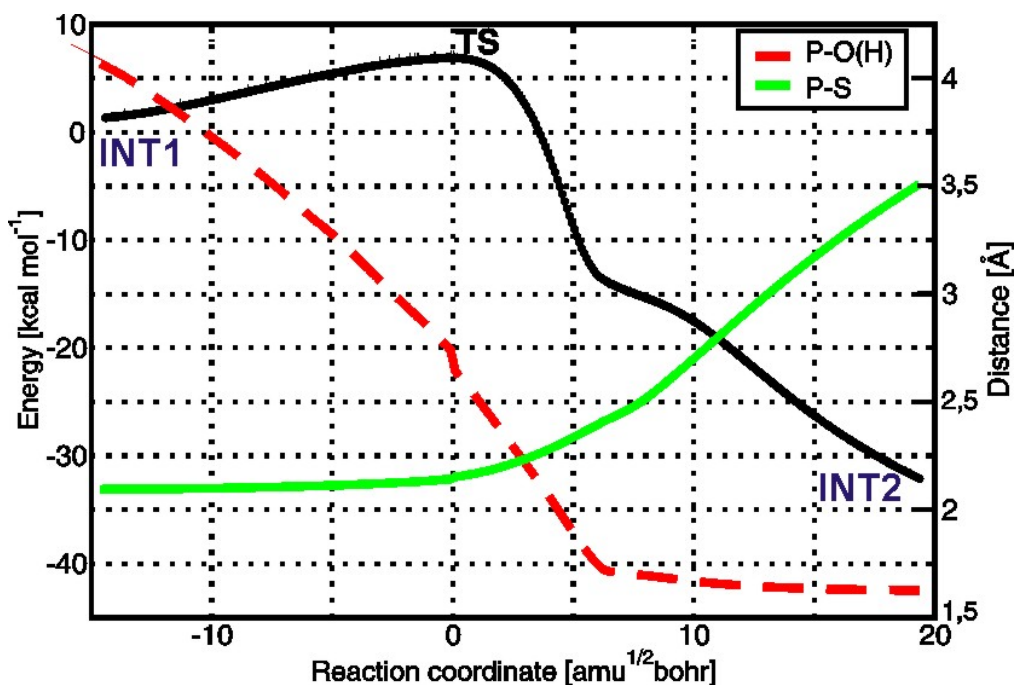
^bMP2/6-311++G(d,p) energy evaluated for structures fully optimized at the same level of theory.

^cMP2/6-311++G(d,p) energy evaluated for structures fully optimized at the HF/6-31+G(d) level of theory; *i.e.* MP2/6-311++G(d,p)//HF/6-31+G(d).

Hydrolysis of demeton-S

Demeton-S undergoes a single-step alkaline hydrolysis according to the direct-displacement mechanism. Below shown is the energy profile as revealed by IRC simulation.

Figure S2: Energy profile for the alkaline hydrolysis of demeton-S. Potential energy changes with respect to separately optimized reactants structure, INT1 (black dotted line; ZPE not included) were generated by HF/6-31+G(d) IRC calculation starting with TS structure (reaction coordinate “0”). Variation in the interatomic distances is given for a phosphorus-hydroxide oxygen as well as phosphorus-sulphur atoms separation.



Comparison of geometries for A and B paths

Below presented are the structures associated with all the stationary points along reaction pathways reported in this contribution.

Figure S3: HF/6–31+G(d) geometries of the stationary points along a reaction coordinate for the alkaline hydrolysis of *O,O*–dimethyl phosphorofluoridate.

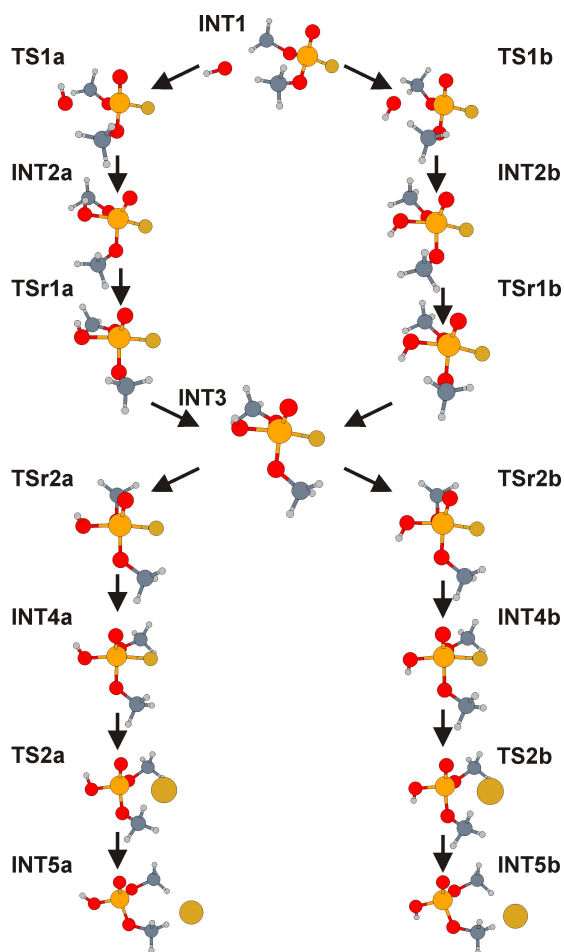


Figure S4: HF/6–31+G(d) geometries of the stationary points along a reaction coordinate for the alkaline hydrolysis of **DFP**.

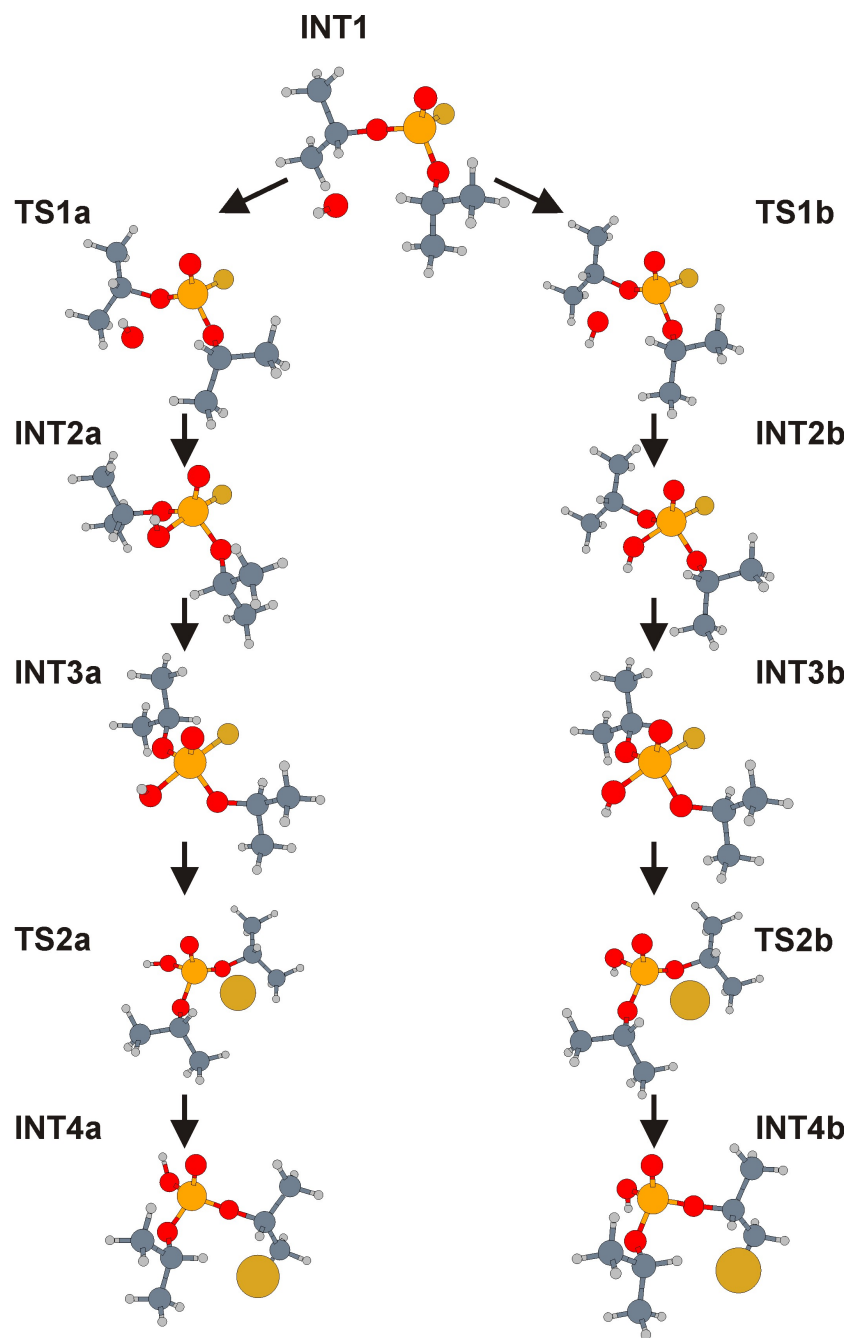


Figure S5: HF/6–31+G(d) geometries of the stationary points along a reaction coordinate for the alkaline hydrolysis of **sarin**.

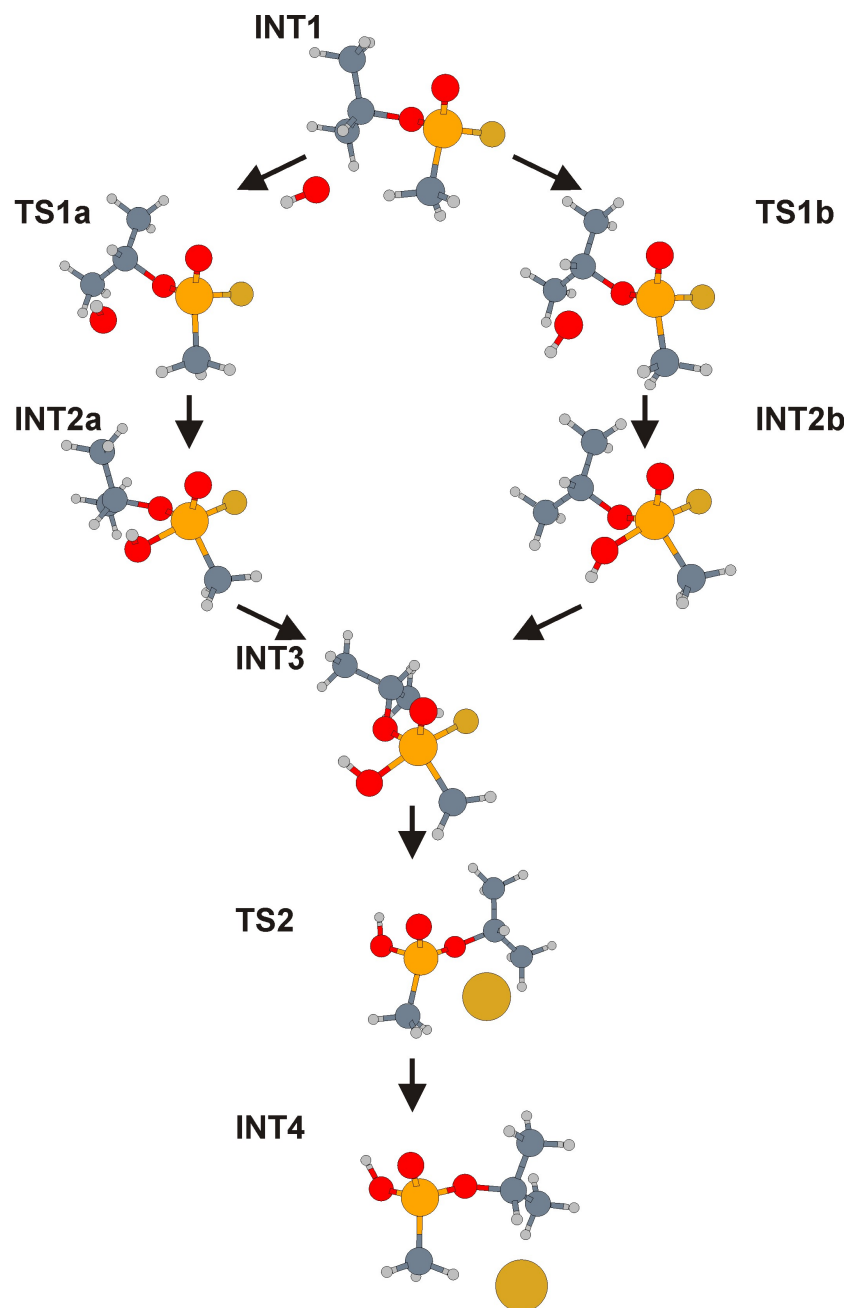


Figure S6: HF/6-31+G(d) geometries of the stationary points along a reaction coordinate for the alkaline hydrolysis of **tabun**.

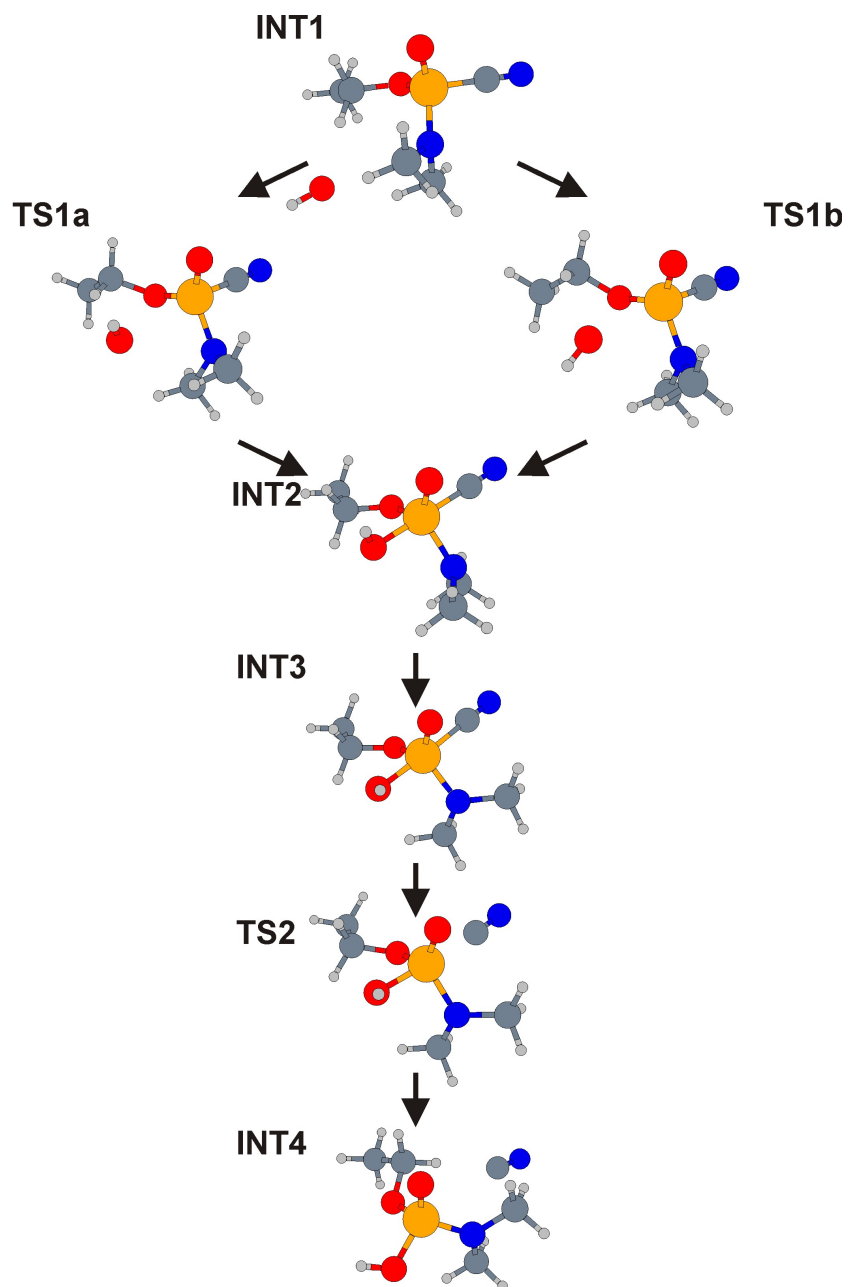


Figure S7: HF/6-31+G(d) geometries of the stationary points along a reaction coordinate for the hydrolysis of **acephate**.

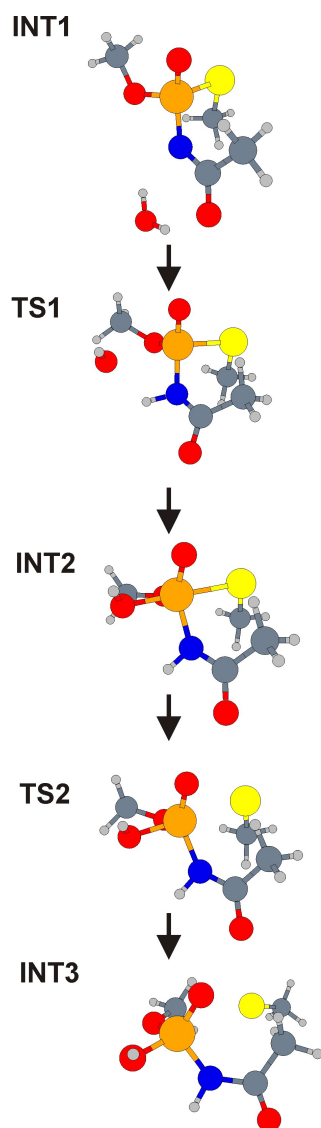


Figure S8: HF/6-31+G(d) geometries of the stationary points along a reaction coordinate for the alkaline hydrolysis of **paraoxon**.

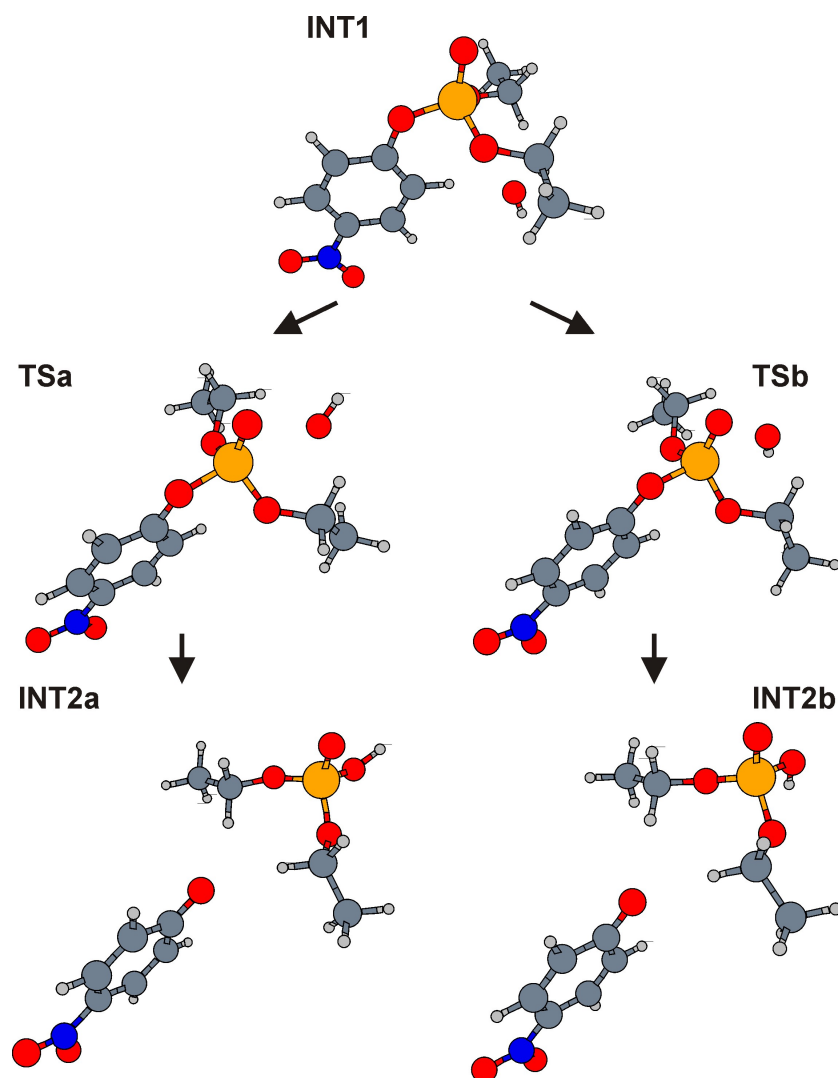


Figure S9: HF/6-31+G(d) geometries of the stationary points along a reaction coordinate for the alkaline hydrolysis of **parathion**.

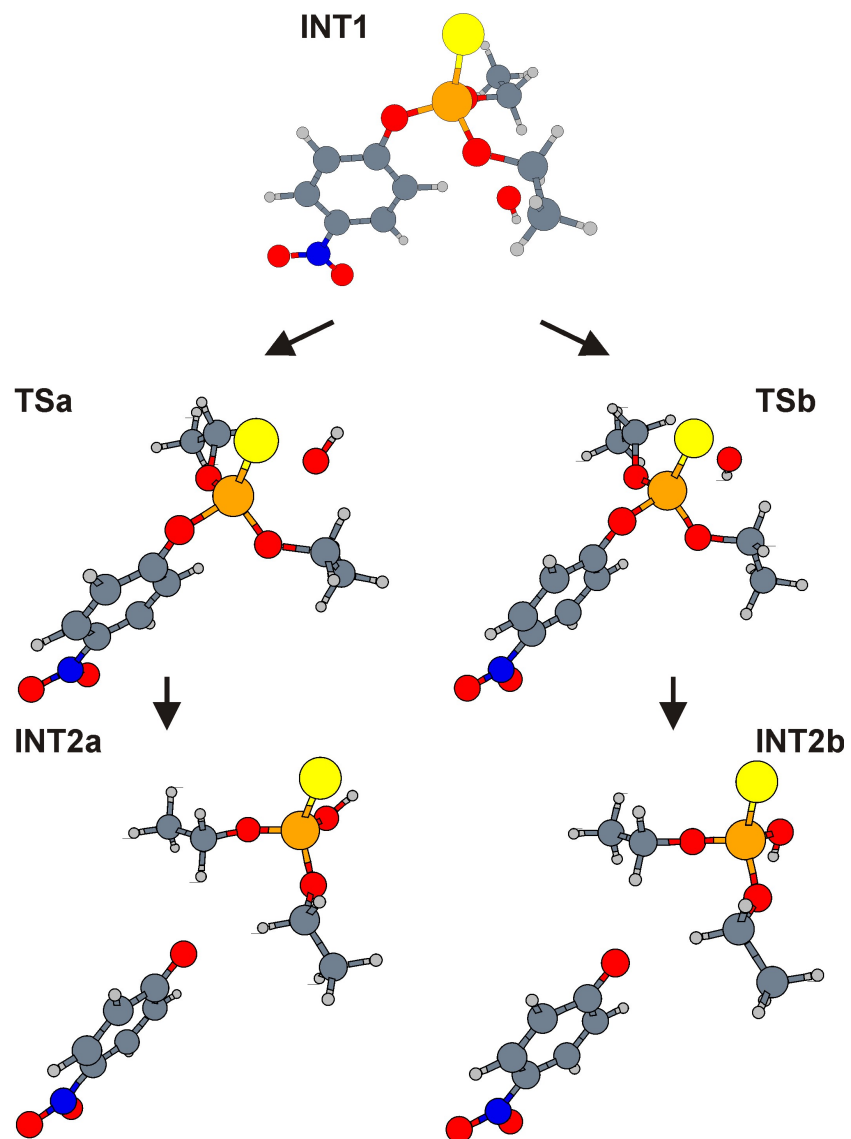
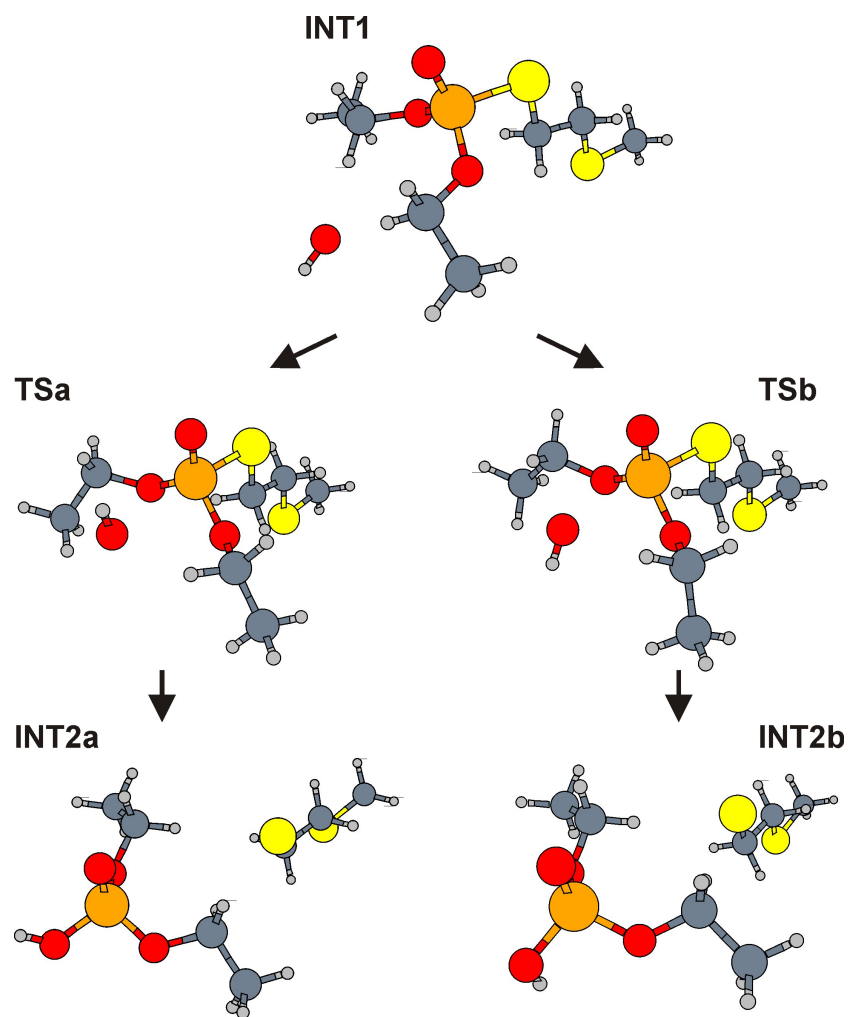


Figure S10: HF/6-31+G(d) geometries of the stationary points along a reaction coordinate for the alkaline hydrolysis of **demeton-S**.



Solvent-induced effects

Influence of the solvent was examined by means of polarizable continuum model, PCM,¹ as applied for gas phase HF/6-31+G(d) geometries. Relative energies associated with alkaline hydrolysis of all the compounds studied herein are given in the Tables S3, S4, and S5.

Table S3: MP2/6-311++G(d,p) relative energies (kcal · mol⁻¹) for the hydrolysis of *O,O*-dimethyl phosphorofluoridate (A and B paths).

	ΔE^{PCM}
INT1→TS1	3.1 (2.7) ^a
INT1→INT2	-19.0 (-16.7)
INT2→TSr1	2.9 (1.2)
INT2→INT3	-1.5 (-3.8)
INT3→TSr2	3.3 (2.5)
INT3→INT4	0.1 (-0.8)
INT4→TS2	0.6 (2.4)
INT4→INT5	-8.9 (-9.1)
INT1→INT5	-29.4 (-30.4)

^aIn parentheses given are the results for B path.

¹Cancés, E.; Mennucci, B.; Tomasi, J. *J. Phys. Chem.* **1996**, *100*, 16502–16513.

Table S4: Relative energies (kcal · mol⁻¹) for the multistep hydrolysis of DFP, sarin, acephate, and tabun (A and B paths) as determined at MP2/6-311++G(d,p)//HF/6-31+G(d) level of theory.

		ΔE^{PCM}
DFP	INT1→TS1	3.4 (0.6) ^a
	INT1→INT2	-17.3 (-14.7)
	INT2→INT3	-1.1 (-4.7)
	INT3→TS2	0.5 (1.9)
	INT3→INT4	-10.2 (-10.1)
	INT1→INT4	-28.5 (-29.5)
sarin	INT1→TS1	3.1 (3.1)
	INT1→INT2	-12.9 (-11.5)
	INT2→INT3	-3.0 (-4.5)
	INT3→TS2	-2.3
	INT3→INT4	-11.6
	INT1→INT4	-27.5
tabun	INT1→TS1	4.6 (4.9)
	INT1→INT2	-16.4
	INT2→INT3	-0.9
	INT3→TS2	0.1
	INT3→INT4	-22.4
	INT1→INT4	-39.7
acephate	INT1→TS1 ^b	33.4
	INT1→INT2	17.7
	INT2→TS2	1.3
	INT2→INT3	-13.1
	INT1→INT3	4.6

^aIn parentheses given are the results for B path.

^bResults for the first step of acephate hydrolysis correspond to the reaction between a water molecule and a deprotonated acephate.

Table S5: Relative energies (kcal · mol⁻¹) for the single-step hydrolysis of paraoxon, parathion, and demeton-S (A and B paths) as determined at MP2/6-311++G(d,p)//HF/6-31+G(d) level of theory.

		ΔE^{PCM}
paraoxon	INT1→TS	6.2 (4.9) ^a
	INT1→INT2	-32.3 (-33.1)
parathion	INT1→TS	7.1 (5.3)
	INT1→INT2	-31.1 (-31.8)
demeton-S	INT1→TS	9.1 (7.2)
	INT1→INT2	-29.1 (-29.8)

^aIn parentheses given are the results for B path.

Animation of the reaction pathways

In addition to the three reaction trajectories available as a part of the article in the form of Web Enhanced Objects, the following movie composed of the structures obtained during HF/6–31+G(d) IRC simulation has been prepared:

- **model_pathB_IRC.mpg** — the entire reaction pathway for the alkaline hydrolysis of *O,O*–dimethyl phosphorofluoridate (B path); 2.7MB file

All these movies are also available at the following location:

http://www.mml.ch.pwr.wroc.pl/edytad/CWA_trajectories.html